

Synthesis and In-Vivo Evaluation of [^{11}C]p-PVP-MEMA as a PET Radioligand for Imaging Nicotinic Receptors

Frédéric Dollé,^A Sandrine Langle,^A Gaëlle Roger,^A Roger R. Fulton,^B Béatrice Lagnel-de Bruin,^A David J. Henderson,^B Françoise Hinnen,^A Taliesha Paine,^C Mark J. Coster,^D Heric Valette,^A Michel Bottlaender,^A and Michael Kassiou^{C,E,F,G}

^ACEA, Service Hospitalier Frédéric Joliot, Institut d'Imagerie Biomédicale, 4 Place du Général Leclerc, F-91401 Orsay, France.

^BDepartment of PET and Nuclear Medicine, Royal Prince Alfred Hospital, Missenden Road, Camperdown, NSW 2050, Australia.

^CSchool of Chemistry, University of Sydney, NSW 2006, Australia.

^DEskitis Institute for Cell and Molecular Therapies, Griffith University, Don Young Rd, Nathan, Qld 4121, Australia.

^EDiscipline of Medical Radiation Sciences, University of Sydney, NSW 2006, Australia.

^FBrain and Mind Research Institute, 100 Mallett St, Camperdown, NSW 2050, Australia.

^GCorresponding author. Email: m.kassiou@usyd.edu.au

Within the class of (4-pyridinyl)vinylpyridines developed by Abbott laboratories as potent neuronal nicotinic acetylcholine receptor ligands, *p*-PVP-MEMA (*(R)*-2-[6-chloro-5-((*E*)-2-pyridin-4-ylvinyl)pyridin-3-yloxy]-1-methylethyl)methylamine) is the lead compound of a novel series that do not display the traditional nicotinic-like pyrrole-ring but still possessing high subnanomolar affinity (K_i 0.077 nM—displacement of [^3H](–)cytisine from whole rat brain synaptic membranes). In the present study, *p*-PVP-MEMA and its nor-derivative (*(R)*-2-[6-chloro-5-((*E*)-2-pyridin-4-ylvinyl)pyridin-3-yloxy]-1-methylethyl)methylamine) as precursor for labelling with the short-lived positron-emitter carbon-11 ($T_{1/2}$ 20.4 min) were synthesized in 10 chemical steps from 2-hydroxy-5-nitropyridine and Boc-D-alanine. *N*-Alkylation of nor-*p*-PVP-MEMA with [^{11}C]methyl iodide afforded [^{11}C]p-PVP-MEMA (>98% radiochemically pure, specific activity of 86.4 GBq μmol^{-1}) in 2% (non-decay corrected and non-optimized) radiochemical yield, in 34 min (including HPLC purification and formulation). Preliminary positron emission tomography (PET) results obtained in a *Papio hamadryas* baboon showed that [^{11}C]p-PVP-MEMA is not a suitable PET-radioligand.

Manuscript received: 27 February 2008.

Final version: 22 April 2008.

1. Introduction

Nicotinic receptors play an important role in complex brain functions, such as learning and memory, and they are also involved in the pathogenesis of several brain disorders, such as Alzheimer's disease, Parkinson's disease, Tourette's syndrome, schizophrenia, depression, and attention deficit/hyperactivity disorder.^[1–3] It is without dispute that dementia is an increasingly important health problem in this century. Alzheimer's disease is the most common type of dementia, but frontotemporal and diffuse Lewy body disease are increasingly being recognized as important causes of dementia. Nicotinic cholinergic mechanisms may be important in explaining the pathophysiology and in designing treatments for Alzheimer's disease.^[4] Postmortem studies have shown that patients who have Alzheimer's disease have a marked reduction in neuronal nicotinic acetylcholine receptors (nAChRs) compared with age-matched controls. These losses have been attributed to the major brain nAChR subtype $\alpha 4\beta 2$ and may reflect, in part, the loss of presynaptic receptors from cholinergic forebrain neurones and their terminal processes.^[5] The loss

of nAChRs is found not only in Alzheimer's disease, but also in Parkinson's disease, Lewy body dementia, and progressive supranuclear palsy.^[5]

Important progress in the knowledge of the structure and properties of brain nAChRs has been achieved over the past decade. However, the mechanisms by which they contribute to the pathogenesis of various neuropsychiatric disorders still remain largely unknown. The introduction of non-invasive imaging techniques, such as positron emission tomography (PET) has made possible the study of neuroreceptors in living subjects.

Studies of the localization and quantification of these receptors can offer insight into their status in normal and disease states only when suitable radioligands are developed.^[6–8] To this end a tremendous amount of effort has focussed on analogues of the alkaloid epibatidine (Fig. 1), resulting in the development of several radioligands labelled with either carbon-11 (half-life 20.4 min), fluorine-18 (half-life 109.8 min), and bromine-76 (half-life 16.2 h).^[9–18] Although most of these showed brain distribution and in vivo pharmacological characteristics suitable

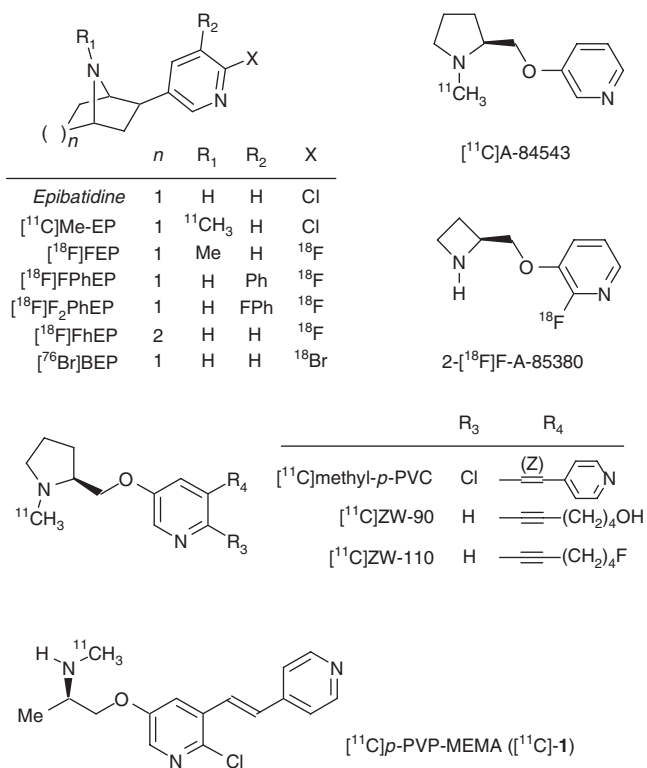


Fig. 1. Selected nicotinic acetylcholine receptor molecules including *p*-PVP-MEMA **1**.

for imaging nAChRs,^[19–23] their toxicity as a result of subtype non-selectivity prohibited their use in humans.^[24]

During the same period a series of 3-pyridyl ether compounds that possess subnanomolar affinity for brain nAChRs with an ability to differentially activate subtypes of neuronal nAChRs were described.^[25] Of these compounds the pyrrolidine-based ligand, A-84543 (*K_i* 0.15 nM) (Fig. 1) was the first to be labelled from this series with carbon-11.^[26] This derivative, which only showed moderate specific binding to nAChRs in vivo in mice and baboon,^[27,28] opened the route to the design of several novel analogues, such as the azetidyl-based fluoropyridine 2-[¹⁸F]F-A-85380,^[29–31] which is currently the only PET probe used in humans for quantitative brain imaging of the nAChRs.^[32–35] More recently analogues of A-84543, such as ZW-90/ZW-110^[36,37] and methyl-*p*-PVC,^[38] have been labelled using carbon-11. All of them have been evaluated in non-human primates using PET, but of particular interest was [¹¹C]methyl-*p*-PVC, a compound that displays a high in vitro nAChR binding (*K_i* 56 pM) and shown to be suitable for studying nAChR occupancy using endogenous and exogenous ligands.^[39]

Further structure–activity relationship studies from this series (performed by Abbott laboratories) have identified structures that do not display the traditional nicotinic-like cyclic pyrrolidine or azetidyl motif but still retain a high affinity for nAChRs.^[40] One of the lead members from this series, {(*R*)-2-[6-chloro-5-((*E*)-2-pyridin-4-ylvinyl)pyridin-3-yloxy]-1-methylethyl}methylamine (*p*-PVP-MEMA, **1**, Fig. 1), possesses high affinity for nAChRs (*K_i* 77 pM)^[40] and also contains a methylamino moiety amenable to radiolabelling using carbon-11 (Fig. 1). This represents an interesting lead molecule as it contains a secondary amine that is in line with the most successful nAChR ligand, 2-[¹⁸F]F-A-85380, and therefore may

possesses superior imaging properties to the tertiary amine pyrrolidine analogue [¹¹C]methyl-*p*-PVC. The aim of the present study was to label *p*-PVP-MEMA with carbon-11 and perform preliminary in vivo assessment in a baboon using PET.

2. Results and Discussion

2.1. Chemistry

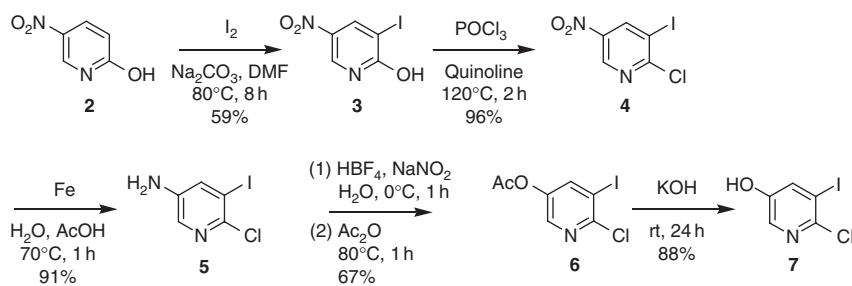
The syntheses of *p*-PVP-MEMA **1** and its corresponding nor-methyl derivative **14**, as a precursor for carbon-11 labelling, are outlined in Schemes 1–3. 2-Chloro-5-hydroxy-3-iodopyridine **7** was obtained in six steps and 30% overall yield from commercially available 2-hydroxy-5-nitropyridine **2**. Briefly, iodination of **2** with iodine and sodium carbonate in *N,N*-dimethylformamide (DMF) at 80°C for 8 h gave the iodopyridine **3** in 59% yield. Chlorination of **3** was performed at 120°C for 2 h using phosphoryl chloride in quinoline and yielded the chloropyridine **4** in 96% yield. Reduction of the nitro function, performed at 70°C for 1 h using iron powder in a 2/3 mixture (v/v) of water and glacial acetic acid, afforded the aminopyridine **5** in 91% yield. Substitution of the amino-function by an acetoxy function was performed using the following two-step sequence: (i) reaction of **5** at 0°C for 1 h in 48% aqueous tetrafluoroboric acid and aqueous sodium nitrite, followed by filtration of the reaction product; and (ii) reaction in acetic anhydride of the obtained crude solid for 1 h at 80°C. 5-Acetoxy-2-chloro-3-iodopyridine **6** was readily obtained in 67% yield and immediately hydrolyzed at room temperature with aq. 2 N potassium hydroxide for 24 h to give the hydroxypyridine **7** in 88% yield (Scheme 1).

N-Boc-D-alanine **8** was reduced with borane tetrahydrofuran complex (1 M in tetrahydrofuran) at 0°C during 2 h to give the corresponding alcohol **9** in 89% yield (Scheme 2). Mitsunobu coupling of **9** and the hydroxypyridine **7** using diisopropyl azodicarboxylate (1.2 equiv.) and triphenylphosphine (1.2 equiv.) in tetrahydrofuran at room temperature for 24 h gave the ether **10** in a moderate yield of 40%. *N*-Methylation of derivative **10** was performed using methyl iodide and sodium hydride in DMF at room temperature for 18 h and afforded **11** in 94% yield.

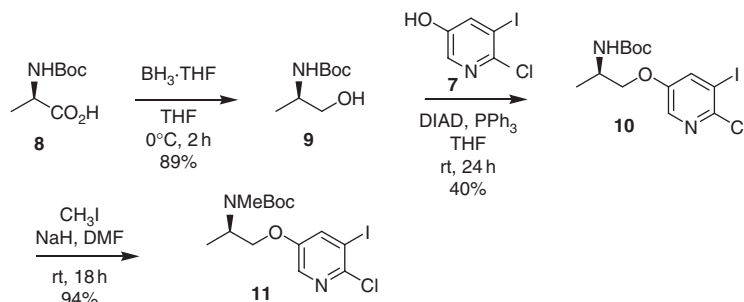
Palladium-catalyzed Heck-type coupling of compounds **10** and **11** with 4-vinylpyridine, using palladium acetate as the catalyst, in acetonitrile that contained tri(*o*-tolyl)phosphine and diisopropylamine at 95°C for 3 h gave the corresponding 2-pyridin-4-ylvinylpyridines **12** and **13** in 45 and 48% yield, respectively (Scheme 3). Finally, *N*-Boc removal was performed with trifluoroacetic acid in dichloromethane (1/5, v/v) at room temperature for 15 min and cleanly gave the amines **14** and **1** in 98 and 93% yield, respectively.

2.2. Radiochemistry

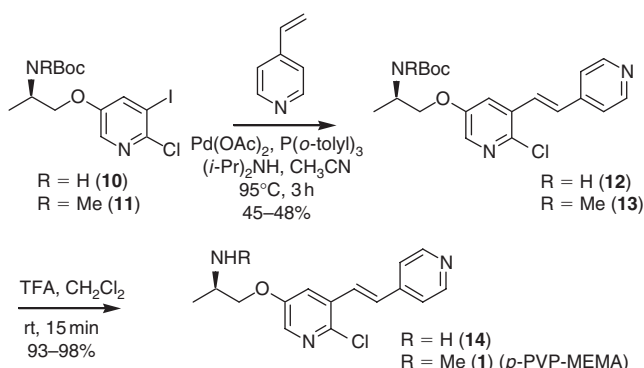
p-PVP-MEMA **1** was labelled with carbon-11 (*T*_{1/2} 20.4 min) using [¹¹C]methyl iodide from the corresponding nor-methyl derivative **14** by *N*-methylation (Scheme 4). [¹¹C]Methyl iodide was synthesized from cyclotron-produced [¹¹C]carbon dioxide, trapped in a DMF solution that contained 14 and tetra-*n*-butylammonium hydroxide and allowed to react at room temperature for 2 min, followed by heating at 80°C for 5 min. The reaction mixture was purified by reverse phase semi-preparative HPLC. This afforded [¹¹C]-**1** in 2% (*n* = 4) non-decay corrected radiochemical yield, based on starting [¹¹C]methyl iodide, in an average synthesis time of 34 min (including HPLC purification and formulation). Co-injection of the non-radioactive **1** was performed using analytical HPLC to confirm the identity of the product. In the final product solution, radiochemical and



Scheme 1. Synthesis of 2-chloro-5-hydroxy-3-iodopyridine **7**.



Scheme 2. Synthesis of [(*R*)-2-(6-chloro-5-iodopyridin-3-yloxy)-1-methylethyl]methylcarbamic acid *tert*-butyl ester **11**.



Scheme 3. Synthesis of nor-*p*-PVP-MEMA **14** and *p*-PVP-MEMA **1**.

chemical purity was greater than 98% with a specific activity of 86.4 GBq μmol^{-1} (2.33 Ci μmol^{-1}). No attempts were made to optimize these conditions as sufficient quantities of the radioligand were produced to enable preliminary pharmacological evaluation.

Formulation of labelled product for intravenous injection was achieved using the following sequence: (i) evaporation of HPLC solvent; (ii) reconstitution of residue in water for injections (4 mL); and (iii) sterile filtration through a 0.22 μm filter. The final injectable solution was clear and colourless with a pH of 7.0. The preparation was free from starting labelling precursor **14**. Administration to the animal was performed within 10 min following the end of synthesis.

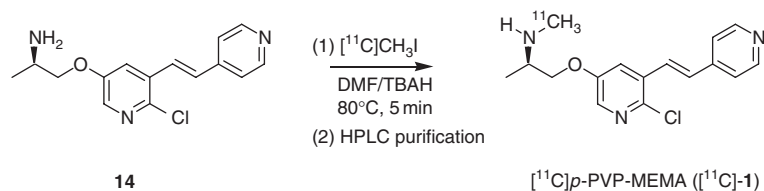
2.3. Evaluation using PET

The in-vivo uptake of [^{11}C]-**1** was examined using PET in a *Papio hamadryas* baboon. Dynamic PET brain imaging commenced just before intravenous administration of [^{11}C]-**1** (100 MBq in 4 mL of saline) and was terminated 60 min post injection.

Figure 2a shows the time activity curves obtained in the thalamus (\blacksquare) and the cerebellum (\square), regions known to contain the highest and lowest density of nAChRs respectively. Brain uptake of [^{11}C]-**1** reached maximal uptake after 2 min (0.4–0.6% of injected dose per 100 mL of tissue (% I.D. 100 mL $^{-1}$)) and stayed at approximately the same uptake level for the remaining 58 min of imaging for both structures. Figure 2b illustrates in a slice containing the thalamus the poor brain penetration of [^{11}C]-**1**. As a result of similar uptake in both regions, the index of specific binding determined as the ratio of thalamus over cerebellum was ~ 1 throughout the time course of the experiment. In contrast, [^{11}C]methyl-*p*-PVC in rhesus monkey has been shown to display a thalamus to cerebellum ratio of around 1.5 at 20 min post-injection, which increases to 4.5 at 90 min.^[39]

3. Conclusion

In this study, *p*-PVP-MEMA **1**, a chemically closely related structure to methyl-*p*-PVC without containing the cyclic pyrrolidine moiety was synthesized, radiolabelled with carbon-11, and evaluated in a baboon using PET. [^{11}C]-**1** was prepared by *N*-alkylation of the nor-methyl derivative **14** with [^{11}C]methyl iodide in reproducible yields and specific radioactivities. The preliminary results from a single PET imaging study revealed that [^{11}C]-**1** uptake in the baboon brain was homogeneous with no amplification in regions known to contain a high density of nAChRs. There are several possible reasons for this observation including the metabolic stability of [^{11}C]-**1**. Although this has not been measured it is possible that [^{11}C]-**1** is rapidly metabolized in blood or other peripheral tissue before entering the central nervous system (CNS). Another possible explanation is that [^{11}C]-**1** could also be a substrate for P-glycoprotein (P-gp) and prevents its entry into the CNS. Another less likely explanation is the lipophilicity (log P) of [^{11}C]-**1**. It has been reported that CNS ligands should possess a log P of between 2 and 3.5 for maximal CNS penetration. [^{11}C]-**1** possesses a calculated log P of 2.8 which



Scheme 4. Radiosynthesis of [¹¹C]*p*-PVP-MEMA [¹¹C]-1.

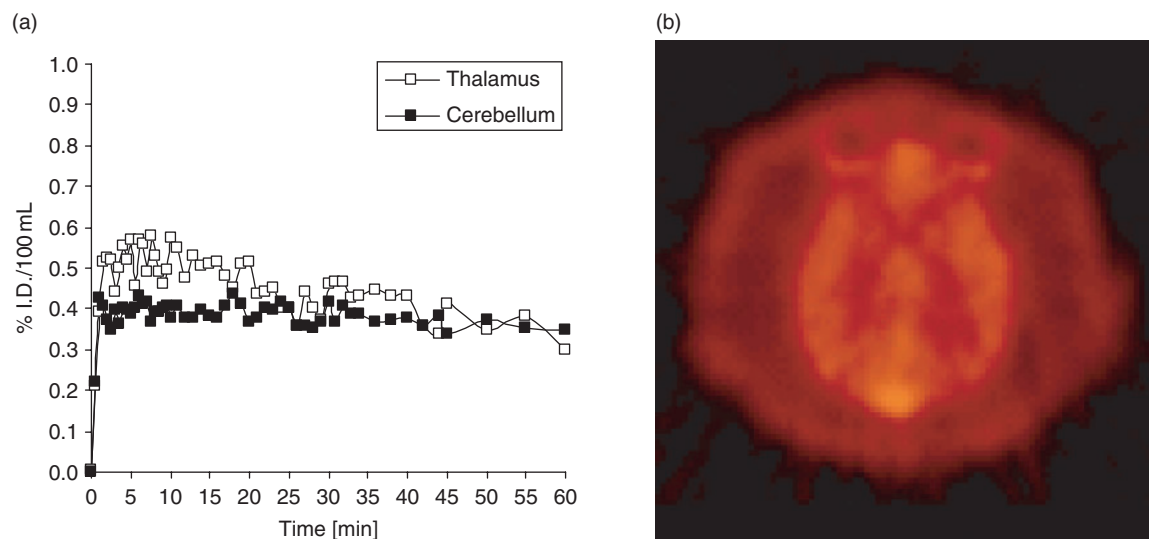


Fig. 2. PET imaging of [¹¹C]*p*-PVP-MEMA [¹¹C]-1 in a *Papio hamadryas* baboon. (a) Time activity curves of [¹¹C]-1 in the thalamus (■, a nAChR-rich region) and the cerebellum (□, a nAChR-poor region), (b) Activity distribution in a slice containing the thalamus (at 30–60 min).

would suggest that it is within the expected range. However, a comprehensive theory of the relationship between lipophilicity and imaging characteristics for nAChR radioligands remains to be developed. In spite of its subnanomolar in-vitro affinity for nAChRs, *p*-PVP-MEMA **1** does not possess the required properties for studying nAChRs in the brain using PET.

4. Experimental

4.1. General

4.1.1. Chemicals, TLC, and HPLC

Chemicals were purchased from Aldrich, Fluka, or Sigma France and were used without further purification. TLCs were run on pre-coated plates of silica gel 60F₂₅₄ (Merck). The compounds were visualized when possible at 254 nm using a UV-lamp and/or by dipping the TLC plates in a 1% ethanolic ninhydrin solution and heating on a hot plate. HPLCs were performed using the following columns and conditions: HPLC A: semi-preparative column, Symmetry C18 (300 × 7.8 mm, 7 μm); eluent 70/30/0.1 (v/v/v) acetonitrile/water/NEt₃; flow rate 7.0 mL min⁻¹. HPLC B: semipreparative X-Terra RP C18 column (300 × 7.8 mm, 10 μm); eluent 30/70 (v/v) acetonitrile/0.1 M aq. NH₄OAc (adjusted to pH 10); flow rate 6.0 mL min⁻¹. HPLC C: analytical X-Terra RP C18 column (150 × 4.6 mm, 5 μm); eluent 20/80 (v/v) acetonitrile/0.1 M aq. NH₄OAc (adjusted to pH 7); flow rate 2.0 mL min⁻¹.

4.1.2. Spectroscopy

NMR spectra were recorded on a Bruker Avance 400 MHz apparatus using the hydrogenated residue of the deuterated

solvents (CD₂Cl₂, δ 5.32; CDCl₃, δ 7.24; (D₆)acetone, δ 2.05) and/or TMS as internal standards for ¹H NMR spectra as well as the deuterated solvents (CD₂Cl₂, δ 53.8; CDCl₃, δ 77.2) and/or TMS as internal standards for ¹³C NMR spectra. Chemical shifts are reported in ppm, downfield from TMS (s, d, t, dd, m, and br for singlet, doublet, triplet, doublet of doublet, multiplet, and broad, respectively). Mass spectra (MS), DCI/NH₄⁺, were measured on a Thermo-Finnigan LCQ Deca XP+ apparatus.

4.2. Chemistry

2-Hydroxy-3-iodo-5-nitropyridine **3**

2-Hydroxy-5-nitropyridine **2** (14.0 g, 0.1 mol, MW 140.10) and Na₂CO₃ (11.0 g, 0.1 mol, 1 equiv., MW 105.99) were dissolved in 100 mL of DMF. Iodine (25.3 g, 0.1 mol, 1 equiv., MW 253.81) was added over 3 min and the reaction mixture was then heated at 80°C for 8 h. The final dark reaction mixture was rotary evaporated to one-half of its initial volume, cooled to room temperature, diluted with water, and filtered. The solution was then made acidic (pH 5) with glacial acetic acid. The resulting yellow solid was filtered off and dried under vacuum to give 15.8 g (59%) of 2-hydroxy-3-iodo-5-nitropyridine **3**. *R*_F 0.30 (heptane/EtOAc, 1/1 (v/v)). δ_H ((D₆)acetone, 298 K) 8.82 (d, *J* 1.5, 1H), 8.75 (d, *J* 1.6, 1H). δ_C ((D₆)acetone, 298 K) 167.7 (C), 163.7 (C), 143.4 (CH), 138.5 (CH), 95.0 (C). *m/z* (C₅H₃IN₂O₃): 267 [M + H]⁺.

2-Chloro-3-iodo-5-nitropyridine **4**

Compound **3** (12.8 g, 48.1 mmol, MW 265.99) dissolved in 6 mL of DMF was added to quinoline (2.9 mL, 24.4 mmol, 0.5 equiv., MW 129.16, *d* 1.093). The reaction flask was cooled

to 5°C, and phosphoryl chloride (4.5 mL, 48.3 mmol, 1 equiv., MW 153.33, *d* 1.645) was added dropwise. The mixture was blanketed with argon and heated at 120°C for 2 h. The mixture was then cooled to room temperature and 15 mL of water added. The mixture was cooled to 0°C and the resulting brown solid was filtered off. Recrystallization from ethanol gave 13.1 g (96%) of 2-chloro-3-iodo-5-nitropyridine **4** as a pale brown solid. *R*_F 0.76 (heptane/EtOAc, 1/1 (v/v)). δ_{H} (CDCl₃, 298 K) 9.17 (d, *J* 1.2, 1H), 8.89 (d, *J* 1.2, 1H). δ_{C} (CD₂Cl₂, 298 K) 160.6 (C), 144.5 (CH), 144.0 (CH), 143.0 (C), 95.0 (C). *m/z* (C₅H₂ClIN₂O₂): 287 [M + H]⁺, 285 [M + H]⁺.

5-Amino-2-chloro-3-iodopyridine **5**

Compound **4** (1.03 g, 3.6 mmol, MW 284.44) was added to a mixture of water (10 mL) and glacial acetic acid (15 mL). Iron powder (849 mg, 15.2 mmol, 4.2 equiv., MW 55.85) was then added to the reaction flask and the mixture was heated for 1 h at 70°C. Once cooled to room temperature, the reaction mixture was diluted with water, and then potassium hydroxide pellets were added until the pH reached >8. The mixture was extracted with EtOAc and the extract evaporated to dryness to yield 841 mg (91%) of 5-amino-2-chloro-3-iodopyridine **5** as a yellow solid. *R*_F 0.46 (heptane/EtOAc, 1/1 (v/v)). δ_{H} (CD₂Cl₂, 298 K) 7.78 (d, *J* 1.2, 1H), 7.48 (d, *J* 1.2, 1H), 3.86 (br s, 2H). δ_{C} (CD₂Cl₂, 298 K) 157.8 (C), 136.1 (CH), 134.2 (CH), 133.3 (C), 94.5 (C). *m/z* (C₅H₄ClIN₂): 257 [M + H]⁺, 255 [M + H]⁺.

5-Acetoxy-2-chloro-3-iodopyridine **6**

Compound **5** (52.0 g, 7.9 mmol, MW 254.46) was dissolved in 11.4 mL of aq. HBF₄ at 0°C. A solution of sodium nitrite (596 mg, 8.6 mmol, 1.1 equiv., MW 69.00) dissolved in 3 mL of water was then added dropwise at 0°C, and the mixture was stirred for another 1 h at 0°C. The resulting solid was filtered off, washed with Et₂O, air-dried, and redissolved in 9.4 mL of acetic anhydride. The reaction mixture was heated for 1 h at 80°C, cooled to room temperature, diluted with EtOH (10 mL), and then concentrated to dryness. EtOH (10 mL) was added again and the mixture concentrated once more to dryness. The resulting solid was dissolved in Et₂O. The organic solution was washed with water, dried with MgSO₄, and concentrated to give 1.57 g (67%) of 5-acetoxy-2-chloro-3-iodopyridine **6** as a pale yellow oil. *R*_F 0.66 (heptane/EtOAc, 1/1 (v/v)). δ_{H} (CD₂Cl₂, 298 K) 8.20 (d, *J* 1.5, 1H), 7.99 (d, *J* 1.5, 1H), 2.30 (s, 3H). δ_{C} (CD₂Cl₂, 298 K) 168.7 (C), 150.9 (C), 145.8 (C), 142.5 (CH), 142.3 (CH), 93.9 (C), 21.0 (CH₃). *m/z* (C₇H₅ClINO₂): 300 [M + H]⁺, 298 [M + H]⁺.

2-Chloro-5-hydroxy-3-iodopyridine **7**

Compound **6** (505 mg, 1.7 mmol, MW 297.48) was dissolved in aq. 2 N KOH (2.55 mL, 3 equiv.) at 5°C. After 24 h at room temperature, the unreacted starting material was removed by filtration. The solution was made acidic (pH 5) by addition of glacial acetic acid and the precipitated 2-chloro-5-hydroxy-3-iodopyridine **7** was filtered off as a white solid (380 mg, 88%). *R*_F 0.56 (heptane/EtOAc, 1/1 (v/v)). δ_{H} ((D₆)acetone, 298 K) 7.98 (d, *J* 1.5, 1H), 7.78 (d, *J* 1.5, 1H), 7.46 (br s, 1H). δ_{C} ((D₆)acetone, 298 K) 154.9 (C), 143.6 (C), 138.1 (CH), 136.4 (CH), 95.0 (C). *m/z* (C₅H₃ClINO): 256 [M + H]⁺, 254 [M + H]⁺.

((R)-2-Hydroxy-1-methylethyl)carbamic Acid tert-Butyl Ester **9**

A solution of BH₃·THF in THF (1 M, 100 mL, 0.1 mol, 1.9 equiv.) was added dropwise to a solution of Boc-D-Ala-OH **8**

(10.0 g, 52.8 mmol, MW 189.21) in 50 mL of THF. The addition occurred over 30 min, and then the reaction mixture was stirred for another 2 h at 0°C. The reaction was quenched with water and the solution was extracted three times with EtOAc. The organic layers were collected, washed with 100 mL of water and 100 mL of brine, dried over anhydrous MgSO₄ and concentrated to dryness to give 8.2 g (89%) of ((R)-2-hydroxy-1-methylethyl)carbamic acid tert-butyl ester **9** as a colourless oil. The solid was used without further purification. *R*_F 0.27 (heptane/EtOAc, 1/1 (v/v)). δ_{H} (CD₂Cl₂, 298 K) 4.70 (br, 1H), 3.72 (br m, 1H), 3.57 (dd, *J* 15.2 and 4.0, 1H), 3.47 (dd, *J* 10.8 and 6.4, 1H), 1.44 (s, 9H), 1.12 (d, *J* 6.8, 3H). δ_{C} (CD₂Cl₂, 298 K) 157.0 (C), 80.0 (C), 67.2 (CH₂), 49.2 (CH), 28.9 (3 × CH₃), 17.9 (CH₃). *m/z* (C₈H₁₇NO₃): 176 [M + H]⁺.

[(R)-2-(6-Chloro-5-iodo-pyridin-3-yloxy)-1-methylethyl]carbamic Acid tert-Butyl Ester **10**

Diisopropyl azodicarboxylate (0.43 mL, 2.2 mmol, 1.2 equiv., MW 202.21, *d* 1.027) and triphenylphosphine (568 mg, 2.2 mmol, 1.2 equiv., MW 262.29) were dissolved in 5 mL of THF at 0°C under argon. Compound **9** (316 mg, 1.8 mmol, MW 175.23) and 2-chloro-5-hydroxy-3-iodopyridine (**7**) (553 mg, 2.2 mmol, 1.2 equiv., MW 255.44) were added to the reaction flask, and the mixture was stirred at room temperature for 24 h. The solvent was evaporated and the crude oil was chromatographed on silica gel using heptane/EtOAc (9/1 to 7/3) to afford 297 mg (40%) of [(R)-2-(6-chloro-5-iodo-pyridin-3-yloxy)-1-methylethyl]carbamic acid tert-butyl ester **10** as a yellow oil. *R*_F 0.65 (heptane/EtOAc, 1/1 (v/v)). δ_{H} (CD₂Cl₂, 298 K) 8.03 (d, *J* 3.1, 1H), 7.71 (d, *J* 2.4, 1H), 5.04 (br s, 1H), 4.05–3.85 (m, 3H), 1.41 (s, 9H), 1.24 (d, *J* 6.7, 3H). δ_{C} (CD₂Cl₂, 298 K) 155.4 (C), 154.1 (C), 145.7 (C), 136.8 (CH), 134.6 (CH), 94.3 (C), 79.5 (C), 72.3 (CH₂), 45.9 (CH), 28.5 (3 × CH₃), 17.7 (CH₃). *m/z* (C₁₃H₁₈ClIN₂O₃): 415 [M + H]⁺, 413 [M + H]⁺.

[(R)-2-(6-Chloro-5-iodopyridin-3-yloxy)-1-methylethyl]methylcarbamic Acid tert-Butyl Ester **11**

To a solution of compound **10** (525 mg, 1.3 mmol, MW 412.65) in 12 mL of DMF at 0°C under argon was added CH₃I (0.63 mL, 10.1 mmol, 8 equiv., MW 141.94, *d* 2.28) followed by NaH (95%, 61 mg, 2.5 mmol, 2 equiv., MW 24.00). The reaction mixture was stirred overnight at room temperature. After careful addition of water, the mixture was extracted three times with Et₂O. The organic layers were collected, dried over anhydrous MgSO₄, and concentrated to dryness. The crude oil was chromatographed on silica gel using heptane/EtOAc (9/1 to 7/3) to afford 511 mg (94%) of [(R)-2-(6-chloro-5-iodopyridin-3-yloxy)-1-methylethyl]methylcarbamic acid tert-butyl ester **11** as a yellow oil. *R*_F 0.63 (heptane/EtOAc, 1/1 (v/v)). δ_{H} (CD₂Cl₂, 298 K) 8.02 (d, *J* 3.0, 1H), 7.70 (d, *J* 2.4, 1H), 4.05–3.80 (m, 3H), 2.75 (s, 3H), 1.42 (s, 9H), 1.21 (d, *J* 7.3, 3H). δ_{C} (CD₂Cl₂, 298 K) 155.8 (C), 154.1 (C), 145.8 (C), 136.8 (CH), 134.6 (CH), 94.2 (C), 79.8 (C), 70.8 (CH₂), 49.8 (CH), 29.5 (CH₃), 28.5 (3 × CH₃), 14.5 (CH₃). *m/z* (C₁₄H₂₀ClIN₂O₃): 429 [M + H]⁺, 427 [M + H]⁺.

{(R)-2-[6-Chloro-5-((E)-2-pyridin-4-ylvinyl)pyridin-3-yloxy]-1-methylethyl}carbamic Acid tert-Butyl Ester **12**

Compound **10** (1.65 g, 4.0 mmol, MW 412.65) was dissolved in 50 mL of acetonitrile. The solution was blanketed with argon. 4-Vinylpyridine (4.8 mL, 44.0 mmol, 11 equiv., MW 105.14, *d* 0.975), diisopropylamine (7 mL, 40.0 mmol, 10 equiv., MW 129.25, *d* 0.742), Pd(OAc)₂ (900 mg, 4.0 mmol, 1 equiv.,

MW 224.49), and P(*o*-tolyl)₃ (1.20 g, 4.0 mmol, 1 equiv., MW 304.38) were successively added to the reaction flask, and the mixture was then stirred for 3 h at 95°C. The solvent was evaporated and the resulting oil was chromatographed on silica gel using heptane/EtOAc (9/1 to 7/3) to afford 708 mg (45%) of {(*R*)-2-[6-chloro-5-((*E*)-2-pyridin-4-yl-vinyl)pyridin-3-yloxy]-1-methylethyl}carbamic acid *tert*-butyl ester **12** as a brown oil. *R*_F 0.16 (heptane/EtOAc, 1/1 (v/v)). δ_H (CD₂Cl₂, 298 K) 8.58 (dd, *J* 4.9 and 1.8, 2H), 8.01 (d, *J* 3.0, 1H), 7.68 (br d, 1H), 7.55 (d, *J* 16.5, 1H), 7.41 (dd, *J* 4.9 and 1.8, 2H), 7.12 (d, *J* 15.8, 1H), 4.91 (br s, 1H), 4.15–3.95 (m, 3H), 1.43 (s, 9H), 1.28 (d, *J* 6.7, 3H). δ_C (CD₂Cl₂, 298 K) 155.6 (C), 155.0 (C), 150.6 (2 × CH), 143.9 (C), 142.0 (C), 137.5 (CH), 131.4 (C), 131.1 (CH), 127.8 (CH), 121.4 (2 × CH), 120.4 (CH), 79.6 (C), 72.2 (CH₂), 45.8 (CH), 28.5 (3 × CH₃), 17.7 (CH₃). *m/z* (C₂₀H₂₄ClN₃O₃): 392 [M + H]⁺, 390 [M + H]⁺.

{(*R*)-2-[6-Chloro-5-((*E*)-2-pyridin-4-ylvinyl)pyridin-3-yloxy]-1-methylethyl}methylcarbamic Acid
tert-Butyl Ester **13**

Compound **11** (235 mg, 0.5 mmol, MW 426.68) was dissolved in 7 mL of acetonitrile. The solution was blanketed with argon. 4-Vinylpyridine (0.65 mL, 6.0 mmol, 11 equiv., MW 105.14, *d* 0.975), diisopropylamine (1 mL, 5.7 mmol, 10 equiv., MW 129.25, *d* 0.742), Pd(OAc)₂ (124 mg, 0.5 mmol, 1 equiv., MW 224.49), and P(*o*-tolyl)₃ (168 mg, 0.5 mmol, 1 equiv., MW 304.38) were successively added to the reaction flask. The mixture was stirred for 3 h at 95°C. The solvent was then evaporated and the resulting oil was chromatographed on silica gel using heptane/EtOAc (9/1 to 7/3 (v/v)) to afford 107 mg (48%) of {(*R*)-2-[6-chloro-5-((*E*)-2-pyridin-4-ylvinyl)pyridin-3-yloxy]-1-methylethyl}methylcarbamic acid *tert*-butyl ester **13** as a yellow oil. *R*_F 0.16 (heptane/EtOAc, 1/1 (v/v)). δ_H (CD₂Cl₂, 298 K) 8.57 (dd, *J* 4.9 and 1.8, 2H), 7.99 (d, *J* 3.1, 1H), 7.63 (br s, 1H), 7.53 (d, *J* 15.9, 1H), 7.40 (dd, *J* 4.8 and 1.8, 2H), 7.10 (br s, 1H), 4.15–3.90 (m, 3H), 2.78 (s, 3H), 1.44 (s, 9H), 1.23 (d, *J* 7.3, 3H). δ_C (CD₂Cl₂, 298 K) 155.9 (C), 154.8 (C), 150.5 (2 × CH), 143.8 (C), 141.9 (C), 137.6 (CH), 131.4 (C), 131.1 (CH), 127.7 (CH), 121.3 (2 × CH), 120.6 (CH), 79.6 (C), 70.5 (CH₂), 49.4 (CH), 29.9 (CH₃), 28.5 (3 × CH₃), 14.5 (CH₃). *m/z* (C₂₁H₂₆ClN₃O₃): 406 [M + H]⁺, 404 [M + H]⁺.

(*R*)-2-[6-Chloro-5-((*E*)-2-pyridin-4-ylvinyl)pyridin-3-yloxy]-1-methylethylamine **14**

To compound **12** (444 mg, 1.1 mmol, MW 389.88) in 5 mL of CH₂Cl₂ was added 1 mL of TFA. The solution was stirred for 15 min at room temperature and concentrated to dryness. The residue was redissolved in 20 mL of CH₂Cl₂ and washed twice with 1 N aq. NaOH. The organic layer was dried over anhydrous MgSO₄ and concentrated to dryness to give 325 mg (98%) of (*R*)-2-[6-chloro-5-((*E*)-2-pyridin-4-ylvinyl)pyridin-3-yloxy]-1-methylethylamine **14** as a brown solid. *R*_F 0.2 (CH₂Cl₂/MeOH, 9/1 (v/v)). δ_H (CD₂Cl₂, 298 K) 8.57 (dd, *J* 4.3 and 1.8, 2H), 8.00 (d, *J* 3.1, 1H), 7.53 (d, *J* 16.4, 1H), 7.52 (d, *J* 3.0, 1H), 7.39 (dd, *J* 4.3 and 1.2, 2H), 7.03 (d, *J* 15.9, 1H), 3.92 (dd, *J* 8.5 and 4.3, 1H), 3.77 (t, *J* 8.5, 1H), 3.34 (m, 1H), 1.86 (br s, 2H), 1.16 (d, *J* 6.7, 3H). δ_H (CD₂Cl₂, 298 K) 155.1 (C), 150.6 (2 × CH), 143.8 (C), 141.9 (C), 137.1 (CH), 131.4 (C), 130.9 (CH), 127.8 (CH), 121.4 (2 × CH), 120.6 (CH), 75.6 (CH₂), 46.5 (CH), 19.7 (CH₃). *m/z* C₁₅H₁₆ClN₃O: 292 [M + H]⁺, 290 [M + H]⁺.

{(*R*)-2-[6-Chloro-5-((*E*)-2-pyridin-4-ylvinyl)pyridin-3-yloxy]-1-methylethyl}methylamine **1**

To compound **13** (107 mg, 0.3 mmol, MW 403.90) in 2 mL of CH₂Cl₂ was added 0.4 mL of TFA. The solution was stirred for 15 min at room temperature and concentrated to dryness. The residue was redissolved in 20 mL of CH₂Cl₂ and washed twice with 1 N aq. NaOH. The organic layer was dried over anhydrous MgSO₄ and concentrated to dryness to give 75 mg (93%) of {(*R*)-2-[6-chloro-5-((*E*)-2-pyridin-4-ylvinyl)pyridin-3-yloxy]-1-methylethyl}methylamine **1** as a pale yellow solid. *R*_F 0.2 (CH₂Cl₂/MeOH, 9/1 (v/v)). *t*_R 7.5–8.0 min (HPLC A). δ_H (CD₂Cl₂, 298 K) 8.56 (dd, *J* 4.3 and 1.2, 2H), 7.98 (d, *J* 2.4, 1H), 7.51 (d, *J* 3.1, 1H), 7.51 (d, *J* 15.9, 1H), 7.37 (dd, *J* 4.3 and 1.8, 2H), 7.01 (d, *J* 16.5, 1H), 4.00–3.80 (m, 2H), 3.05–2.90 (m, 1H), 2.43 (s, 3H), 1.13 (d, *J* 6.7, 3H). δ_C (CD₂Cl₂, 298 K) 155.1 (C), 150.6 (2 × CH), 143.7 (C), 141.8 (C), 137.1 (CH), 131.4 (C), 130.1 (CH), 127.7 (CH), 121.3 (2 × CH), 120.6 (CH), 73.2 (CH₂), 54.3 (CH), 34.0 (CH₃), 16.9 (CH₃). *m/z* (C₁₆H₁₈ClN₃O): 306 [M + H]⁺, 304 [M + H]⁺.

4.3. Radiochemistry

4.3.1. Preparation of [¹¹C]Methyl Iodide

The target gas (N₂ + 0.5% O₂) was bombarded with protons using a 16 MeV cyclotron to produce [¹¹C]CO₂. The [¹¹C]CO₂ was transferred to an automated module and concentrated onto molecular sieves. The sieves were heated to release [¹¹C]CO₂, which was reduced by hydrogen on a nickel catalyst to form [¹¹C]CH₄. The [¹¹C]CH₄ was released into the CH₃I conversion part of the module where it was recirculated through a quartz column (packed with ascarite and iodine crystals) by helium carrier gas. The [¹¹C]CH₃I formed was trapped in ascarite while any unconverted [¹¹C]CH₄ was transferred to waste.

4.3.2. Preparation and Formulation of [¹¹C]p-PVP-MEMA ([¹¹C]-**1**)

Under helium gas flow, the synthesized [¹¹C]CH₃I was delivered to a 1 mL reaction vessel containing **14** (0.9 mg, 0.003 mmol) in DMF (250 μL) and tetrabutylammonium hydroxide (2 μL) and allowed to stand at room temperature for 2 min, followed by heating at 80°C for 5 min. The reaction mixture was diluted with 0.5 mL of HPLC buffer and purified (HPLC B). The radioactive fraction that corresponded to [¹¹C]-**1** (*t*_R: 8.6 min) was collected and evaporated under vacuum. The residue was reconstituted in sterile water for injections BP (4 mL) and filtered through a sterile Millipore GS 0.22 μm filter into a sterile pyrogen-free evacuated vial.

4.3.3. Quality Control of [¹¹C]p-PVP-MEMA ([¹¹C]-**1**)

For determination of specific radioactivity and radiochemical purity, an aliquot of the final radioactive solution and was injected onto an analytical reverse-phase HPLC column (HPLC C, *t*_R 2.9 min). The area of the UV absorbance peak measured at 254 nm, which corresponded to the carrier product, was measured (integrated) on the HPLC chromatogram and compared with a standard curve relating mass to UV absorbance. The radioactivity of the collected product was measured and divided by the found mass to give the specific radioactivity.

4.4. PET Studies

4.4.1. Animal

A male *Papio hamadryas* baboon aged 13 years and weighing 26.5 kg was selected for PET scanning. The baboon was

maintained and handled in accordance with the NHMRC code of practice for the care and use of non-human primates for scientific purposes. The project application was approved by the Sydney South West Area Health Service (SSWAHS) Animal Ethics Committee. The radioligand injected dose was 100 MBq.

4.4.2. Baboon PET Imaging

All PET data were acquired using a Siemens Biograph LSO PET-CT scanner in the Department of PET and Nuclear Medicine at Royal Prince Alfred Hospital. This dual modality device has a fully three-dimensional (3D) PET scanner with 24 crystal rings and a dual slice CT scanner in the same gantry. It yields a reconstructed PET spatial resolution of 6.3 mm FWHM (full width at half maximum) at the centre of the field of view. A CT scan of the head was completed before radioligand injection. The baboon was initially anaesthetized with ketamine (8 mg kg⁻¹, im). Anaesthesia was maintained with the use of an intravenous infusion of ketamine (Parnell Laboratory, Australia) in saline at a dose rate of 0.2 mg of ketamine kg⁻¹ min⁻¹. The baboon also received MgSO₄ (2 mL intravenous injection of a 2.47 g per 5 mL solution) given over half an hour plus atropine (1 mg im) plus maxalon (5 mg im). The head of the baboon was immobilized with plastic tape to minimize motion artefacts. Acquisition of the PET data in list mode was commenced just before radioligand injection and continued for a period of 60 min. At the conclusion of the study the list mode data were sorted into a dynamic scan comprising 54 frames (20 × 30 s, 30 × 60 s, and 4 × 300 s). The dynamic 3D PET sinograms were rebinned using FORE (Fourier rebinning) and reconstructed with filtered backprojection and CT databased corrections for photon attenuation and scatter into 47 transaxial slices, each comprising 128 × 128 voxels. Reconstructed voxel dimensions were 0.206 × 0.206 × 0.337 cm³. The radioligand uptake was converted into units of percent injected dose per volume of 100 mL of brain tissue (% I.D./100 mL) and plotted against time. An automated 3D registration algorithm was used to co-register the two reconstructed scans before region of interest (ROI) definition. Decay corrected time activity curves representing the variation in ligand concentration versus time were constructed from selected slices for regions of interest over the thalamus and cerebellum.

Acknowledgements

The authors thank Dr Dirk Roeda for proofreading the manuscript. This work was supported by DEST and the French Embassy in Australia under the FAST program (FR040051).

References

- [1] M. Aceto, B. Martin, *Med. Res. Rev.* **1982**, *2*, 43. doi:10.1002/MED.2610020104
- [2] A. Nordberg, H. Lundqvist, P. Hartig, A. Lilja, B. Långström, *J. Neurosci. Res.* **1995**, *31*, 103. doi:10.1002/JNR.490310115
- [3] O. K. Steinlein, J. Stoodt, R. A. de Vos, E. N. Steur, A. Wevers, U. Schutz, H. Schroder, *Neuroreport* **1999**, *10*, 2919.
- [4] J. James, A. Nordberg, *Behav. Genet.* **1995**, *25*, 149. doi:10.1007/BF02196924
- [5] U. Warpman, A. Nordberg, *Neuroreport* **1995**, *6*, 2419. doi:10.1097/00001756-199511270-00033
- [6] D. Gündisch, *Curr. Pharm. Des.* **2000**, *6*, 1143. doi:10.2174/1381612003399879
- [7] W. Sihver, A. Nordberg, B. Långström, A. Mukhin, A. Koren, A. Kimes, E. London, *Behav. Brain Res.* **2000**, *113*, 143. doi:10.1016/S0166-4328(00)00209-6
- [8] A. G. Horti, V. L. Villemagne, *Curr. Pharm. Des.* **2006**, *12*, 3877. doi:10.2174/138161206778559605
- [9] A. G. Horti, H. T. Ravert, E. D. London, R. F. Dannals, *J. Label. Compd Radiopharm.* **1996**, *38*, 355. doi:10.1002/(SICI)1099-1344(199604)38:4<355::AID-JLCR842>3.0.CO;2-3
- [10] Y. S. Ding, S. J. Gatley, J. S. Fowler, N. D. Volkow, D. Aggarwal, J. Logan, S. L. Dewey, F. Liang, F. I. Carroll, M. J. Kuhar, *Synapse* **1996**, *24*, 403. doi:10.1002/(SICI)1098-2396(199612)24:4<403::AID-SYN8>3.0.CO;2-H
- [11] F. Liang, H. A. Navarro, P. Abraham, P. Kotian, Y. S. Ding, J. S. Fowler, N. D. Volkow, M. J. Kuhar, F. I. Carroll, *J. Med. Chem.* **1997**, *40*, 2293. doi:10.1021/JM970187D
- [12] A. G. Horti, U. Scheffel, A. S. Kimes, J. L. Musachio, H. T. Ravert, W. B. Mathews, Y. Zhan, P. A. Finley, E. D. London, R. F. Dannals, *J. Med. Chem.* **1998**, *41*, 4199. doi:10.1021/JM980233P
- [13] J. T. Patt, J. E. Spang, G. Westera, A. Buck, P. A. Schubiger, *Nucl. Med. Biol.* **1999**, *26*, 165. doi:10.1016/S0969-8051(98)00084-5
- [14] L. Dolci, F. Dollé, H. Valette, F. Vaufrey, C. Fuseau, M. Bottlaender, C. Crouzel, *Bioorg. Med. Chem.* **1999**, *7*, 467. doi:10.1016/S0968-0896(98)00261-2
- [15] M. Kassiou, C. Loc'h, F. Dollé, J. L. Musachio, L. Dolci, C. Crouzel, R. F. Dannals, B. Mazière, *Appl. Radiat. Isot.* **2002**, *57*, 713. doi:10.1016/S0969-8043(02)00187-2
- [16] W. Deuther-Conrad, J. T. Patt, D. Feuerbach, F. Wegner, P. Brust, J. Steinbach, *Il Farmaco* **2004**, *59*, 785. doi:10.1016/J.FARMAC.2004.07.004
- [17] G. Roger, W. Saba, H. Valette, F. Hinnen, C. Coulon, M. Ottaviani, M. Bottlaender, F. Dollé, *Bioorg. Med. Chem.* **2006**, *14*, 3848. doi:10.1016/J.BMC.2006.01.032
- [18] G. Roger, F. Hinnen, H. Valette, W. Saba, M. Bottlaender, F. Dollé, *J. Label Compd Radiopharm.* **2006**, *49*, 489. doi:10.1002/JLCR.1063
- [19] V. L. Villemagne, A. G. Horti, U. Scheffel, H. T. Ravert, P. Finley, D. J. Clough, E. D. London, H. N. Wagner, R. F. Dannals, *J. Nucl. Med.* **1997**, *38*, 1737.
- [20] Y. S. Ding, P. E. Molina, J. S. Fowler, J. Logan, N. D. Volkow, M. J. Kuhar, F. I. Carroll, *Nucl. Med. Biol.* **1999**, *26*, 139. doi:10.1016/S0969-8051(98)00070-5
- [21] Y. S. Ding, J. Logan, R. Bermel, V. Garza, O. Rice, J. S. Fowler, N. D. Volkow, *J. Neurochem.* **2000**, *74*, 1514. doi:10.1046/J.1471-4159.2000.0741514.X
- [22] M. Kassiou, M. Bottlaender, C. Loc'h, F. Dollé, J. L. Musachio, C. Coulon, M. Ottaviani, R. F. Dannals, B. Mazière, *Synapse* **2002**, *45*, 95. doi:10.1002/SYN.10087
- [23] H. Valette, F. Dollé, W. Hassoun, G. Roger, F. Hinnen, C. Coulon, M. Ottaviani, A. Syrota, M. Bottlaender, *Synapse* **2007**, *61*, 764. doi:10.1002/SYN.20426
- [24] E. P. Molina, Y. S. Ding, F. I. Carroll, F. Liang, N. D. Volkow, N. Pappas, M. J. Kuhar, N. Abumrad, S. J. Gatley, J. S. Fowler, *Nucl. Med. Biol.* **1997**, *24*, 743. doi:10.1016/S0969-8051(97)00120-0
- [25] M. Abreo, N. Lin, D. Garvey, D. Gunn, A. Hettlinger, J. Wasicak, P. Pavlik, Y. Martin, D. L. Donnelly-Roberts, D. J. Anderson, J. P. Sullivan, M. Williams, S. P. Arneric, M. W. Holladay, *J. Med. Chem.* **1996**, *39*, 817. doi:10.1021/JM9506884
- [26] M. Kassiou, H. T. Ravert, W. B. Mathews, J. L. Musachio, E. D. London, R. F. Dannals, *J. Label. Comp. Radiopharm.* **1997**, *39*, 425. doi:10.1002/(SICI)1099-1344(199705)39:5<425::AID-JLCR984>3.0.CO;2-R
- [27] M. Kassiou, U. A. Scheffel, H. T. Ravert, W. B. Mathews, J. L. Musachio, E. D. London, R. F. Dannals, *Life Sci.* **1998**, *63*, 13. doi:10.1016/S0024-3205(98)00240-9
- [28] F. Yokoi, J. L. Musachio, J. Hilton, M. Kassiou, H. T. Ravert, W. B. Mathews, R. F. Dannals, M. Stephane, D. F. Wong, *J. Nucl. Med.* **1999**, *40*, 263P.
- [29] A. G. Horti, A. O. Koren, H. T. Ravert, J. L. Musachio, W. B. Mathews, E. D. London, R. F. Dannals, *J. Label. Comp. Radiopharm.* **1998**, *41*, 309. doi:10.1002/(SICI)1099-1344(199804)41:4<309::AID-JLCR78>3.0.CO;2-I
- [30] F. Dollé, H. Valette, M. Bottlaender, F. Hinnen, F. Vaufrey, I. Guenther, C. Crouzel, *J. Label. Comp. Radiopharm.* **1998**, *41*, 451.

- doi:10.1002/(SICI)1099-1344(199805)41:5<451::AID-JLCR111>3.0.CO;2-R
- [31] F. Dollé, L. Dolci, H. Valette, F. Hinnen, F. Vaufrey, I. Guenther, C. Fuseau, C. Coulon, M. Bottlaender, C. Crouzel, *J. Med. Chem.* **1999**, *42*, 2251. doi:10.1021/JM9910223
- [32] A. S. Kimes, A. G. Horti, E. D. London, S. I. Chefer, C. Contoreggi, M. Ernst, P. Friello, A. O. Koren, V. Kurian, J. A. Matochik, O. Pavlova, D. B. Vaupel, A. G. Mukhin, *FASEB J.* **2003**, *17*, 1331.
- [33] S. Mitkovski, V. L. Villemagne, K. E. Novakovic, G. O'Keefe, H. Tochon-Danguy, R. S. Mulligan, K. L. Dickinson, T. Saunder, M. Gregoire, M. Bottlaender, *Nucl. Med. Biol.* **2005**, *32*, 585. doi:10.1016/J.NUCMEDBIO.2005.04.013
- [34] J. D. Gallezot, M. Bottlaender, M. C. Grégoire, D. Roumenov, J. R. Deverre, C. Coulon, M. Ottaviani, F. Dollé, A. Syrota, H. Valette, *J. Nucl. Med.* **2005**, *46*, 240.
- [35] J. D. Gallezot, M. Bottlaender, J. Delforge, H. Valette, W. Saba, F. Dollé, C. Coulon, M. Ottaviani, F. Hinnen, A. Syrota, M.-C. Grégoire, *J. Cereb. Blood Flow Metab.* **2008**, *28*, 172. doi:10.1038/SJ.JCBFM.9600505
- [36] M. Kassiou, S. K. Chellappan, D. Henderson, R. Fulton, N. Giboreau, Y. Xiao, Z. L. Wei, D. Guilloteau, P. Emond, F. Dollé, K. J. Kellar, A. P. Kozikowski, *J. Label. Comp. Radiopharm.* **2007**, *50*, S357.
- [37] A. P. Kozikowski, S. K. Chellappan, D. Henderson, R. Fulton, N. Giboreau, Y. Xiao, Z. L. Wei, D. Guilloteau, P. Emond, F. Dollé, K. J. Kellar, M. Kassiou, *ChemMedChem* **2007**, *2*, 54. doi:10.1002/CMDC.200600220
- [38] L. L. Brown, S. Kulkarni, O. A. Pavlova, A. O. Koren, A. G. Mukhin, A. H. Newman, A. G. Horti, *J. Med. Chem.* **2002**, *45*, 2841. doi:10.1021/JM010550N
- [39] L. Brown, S. Chefer, O. Pavlova, D. B. Vaupel, A. O. Koren, A. S. Kimes, A. G. Horti, A. G. Mukhin, *J. Neurochem.* **2004**, *91*, 600. doi:10.1111/J.1471-4159.2004.02762.X
- [40] N. H. Lin, L. Dong, W. H. Bunnelle, D. J. Anderson, M. Meyer, *Bioorg. Med. Chem. Lett.* **2002**, *12*, 3321. doi:10.1016/S0960-894X(02)00740-0